Dislocation Contrast Analysis in Weak Beam Synchrotron X-Ray Topography

Hongyu Peng[1,a*], Zeyu Chen[1,b], Yafei Liu[1,c], Qianyu Cheng[1,d],
Shanshan Hu[1,e], Xianrong Huang[2,f], Lahsen Assoufid[2,g],
Balaji Raghothamachar[1,h] and Michael Dudley[1,i]

[1]Materials Science and Chemical Engineering, Stony Brook University, Stony Brook, New York, 11794, USA

[2]Advanced Photon Source, Argonne National Laboratory, Lemont, Illinois, 60439, USA

[a]hongyu.peng@stonybrook.edu, [b]zeyu.chen@stonybrook.edu, [c]yafei.liu@stonybrook.edu,
[d]qianyu.cheng@stonybrook.edu, [e]shanshan.hu@stonybrook.edu, [f]xiahuang@anl.gov,
[g]assoufid@anl.gov, [h]balaji.raghothamachar@stonybrook.edu
and [i]michael.dudley@stonybrook.edu

Keywords: X-ray Topography, Weak Beam Topography, Dislocation Contrast

Abstract. Synchrotron monochromatic beam X-ray topography has been widely applied to characterize structural defects in SiC crystals. Using ray tracing simulations, the dislocation contrast in X-ray topography under strong diffraction conditions (diffraction takes place at or near Bragg angle) has been intensively investigated. However, the contrast and the configurations of the dislocation images recorded under weak diffraction conditions have not been fully investigated. Recently, we demonstrated that the contrast of dislocations in synchrotron grazing incidence topography under weak diffraction conditions can also be analyzed and interpreted by applying ray tracing principles. In this study, we have extended the application of the ray tracing method to analyze the dislocation contrast in weak beam synchrotron back reflection and rocking curve topography. The ray tracing method is shown to successfully simulate and correlate the contrast of threading screw dislocations at various positions on the rocking curve and thus allow to determine the signs of Burgers vectors.

Introduction

Synchrotron X-ray topography (SXRT) is a non-destructive technique that images structural defects (dislocations, stacking faults, grain boundaries, etc.) in bulk crystals, epitaxial films and wafers fabricated for electronic devices [1-5]. Compared to synchrotron white beam XRT, synchrotron monochromatic beam XRT (SMBXT) shows better defect contrast due to its superior strain sensitivity and signal to noise ratio [6]. In SMBXT (for example grazing incidence topography, back reflection topography and rocking curve topography [7-9]), Bragg contours will typically be formed due to the presence of lattice bending, and the intensity profile across such contours tracks the rocking curve of the crystal. Intensive investigations have been carried out on the dislocation contrast in SMBXT when the diffraction takes place at or near the Bragg angle [6,8,9]. However, the contrast of the dislocations under weak diffraction conditions (i.e. off Bragg contour) reveals additional information since it is more sensitive to the local lattice distortion [7]. Therefore, the understanding of the dislocation contrast in weak beam synchrotron X-ray topography is of great interest.

We have previously reported the dislocation contrast in grazing incidence topography (GIT), and it has been demonstrated that the contrast features under weak diffraction conditions can be described by the orientation contrast mechanism and simulated using the ray tracing method [7]. In this work, the contrast of the dislocations in weak beam synchrotron X-ray back reflection topography and rocking curve topography (RCT) will be presented. Threading screw/mixed dislocations

(TSDs/TMDs) with opposite sign of Burgers vector show different contrast features when they are observed off-contour in back reflection topographs, while previous work has shown that TSDs/TMDs always show circular white contrast in back reflection topographs when they are on-contour, irrespective of sign [6]. Moreover, in synchrotron X-ray RCT, where a beam conditioner is used, the contrast of TSDs/TMDs is more sensitive to the diffraction conditions as the rocking curve width is much narrower. As a result, the contrast of TSDs/TMDs with opposite sign of Burgers vector is dramatically different.

Experiment

The samples studied in back reflection and RCT are (0001) 4H-SiC with 8º and 4º offcut towards [11$\bar{2}$0] respectively. The images in back reflection geometry were recorded using the 000,12 reflection at an energy of 7.5 keV at 33-BM at the Advanced Photon Source (APS) in Argonne National Laboratory, while the 0008 reflection was used in RCT at 1-BM at the APS at an energy of 8 keV.

In back reflection geometry, the monochromator is a double-bounce Si (111) and the full width at half maximum (FWHM) of 4H-SiC 000,12 reflection is calculated to be 30″ according to the DuMond diagram [10]. But the FWHM of 4H-SiC 0008 reflection in RCT is only around 2.4″ since a Si 331 beam conditioner is used in between the sample and the double-bounce Si (111), whose Darwin width is only around 0.48″ calculated from dynamical theory of X-ray diffraction.

To investigate the contrast of the dislocations and determine their Burgers vectors, ray tracing simulations are used in the present work [11], a technique which is originally developed based on the orientation contrast mechanism. In the simulation, the direction of the diffracted X-rays is calculated based on the normal of local diffraction planes, which can be distorted due to the presence of the dislocation. Projecting the diffracted X-rays onto the recording plate as dots, the image of the dislocation is simulated. Moreover, the incident angle is modified based on the location of the dislocation on the contour and the intensity of each dot is described by a simplified rocking curve of the crystal [7], both of which play a key role in the formation of the contrast in weak beam topography.

Results and Discussion

As mentioned in previous section, the intensity profile across the contour in SMBXT tracks the rocking curve of the crystal [7]. Different locations (i.e. different intensities) on the contour represent different incident angles. When the angle is slightly off the Bragg angle, the diffracted intensity will decrease and the contrast on the topograph will be reduced/whiter. A schematic of SiC 000,12 rocking curve is shown in Fig. 1 (a) and nine different diffraction conditions are marked from 'a' to 'i', where position 'e' is the perfect Bragg condition. On the left side of 'e', the incident angle is smaller than Bragg angle (in the experiment, this is caused by the presence of lattice bending), and on the right, the angle is bigger than Bragg angle.

The simulated images of threading screw dislocations (TSDs) under those diffraction conditions are shown in Fig. 1 (b). The Burgers vectors of the dislocation in the first row is right-hand screw while left-hand screw is shown in the second row. It is clear that under strong diffraction condition, 'e', contrast of TSDs with opposite signs of Burgers vectors are indistinguishable. However, the difference between threading right-hand screw dislocation (TRSD) and threading left-hand screw dislocation (TLSD) can be discerned if the incident angle deviates from perfect Bragg angle. Taking diffraction condition 'a' for example, the TRSD shows darker contrast bordering the top right of the white contrast circle while the darker contrast appears to the bottom right for a TLSD (Fig. 1 (b)). Based upon this difference, the sign of Burgers vector can thus be determined in weak beam synchrotron X-ray back reflection topography.

As shown in Fig. 1 (c), the dislocations show circular white contrast in regular on-contour topograph (as marked by the white box). But the contrast of the dislocation gradually changes if moving towards the left side of the contour (as the lattice curvature is concave, the left side of the contour corresponds to the right side of the rocking curve). The two dislocations in the bottom marked by dark boxes have opposite sign of Burgers vectors as the dark contrast of TRSD appears in the bottom left while the dark contrast of TLSD shows on the top left in the boxes, and they are labeled by 'R' and 'L' respectively. But on the right side of the contour (corresponds to the left side of the rocking curve), the dark contrast of TRSD is on the top right while TLSD shows dark contrast in the bottom right in the dark boxes in Fig. 1 (c). Therefore, the sign of Burgers vector that can not be determined in previous on-contour back reflection topography can now be characterized in weak beam synchrotron back reflection topography.
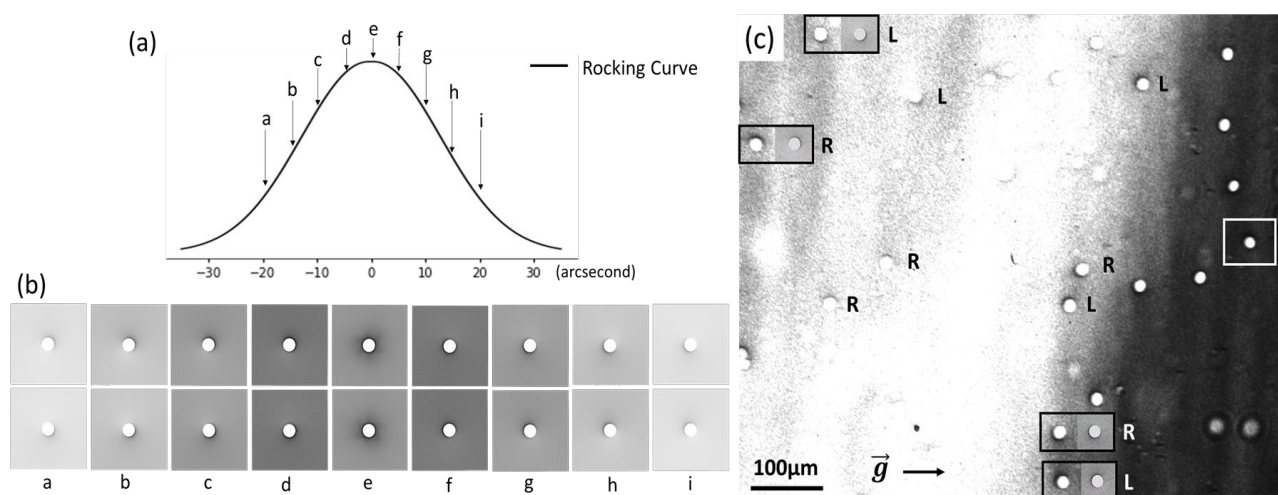

Figure 1. (a) Simplified rocking curve of 4H-SiC in 000,12 back reflection geometry. Nine different diffraction conditions from 'a' to 'i' are marked, where 'e' indicates perfect Bragg condition. (b) Ray tracing simulated image of threading right-hand screw dislocations (TRSD) and threading left-hand screw dislocations (TLSD) are shown in the first and second row, correspondingly to 'a' to 'i' diffraction conditions. Different diffraction conditions are considered. (c) 000,12 Back reflection topograph of 4H-SiC in weak diffraction conditions. Circular white features are threading screw dislocations (TSDs) and simulated images are placed on the right of the topographic images in the boxes. TRSDs are marked by 'R' while TLSDs are marked by 'L'. TSD marked by the white box is under strong diffraction condition.
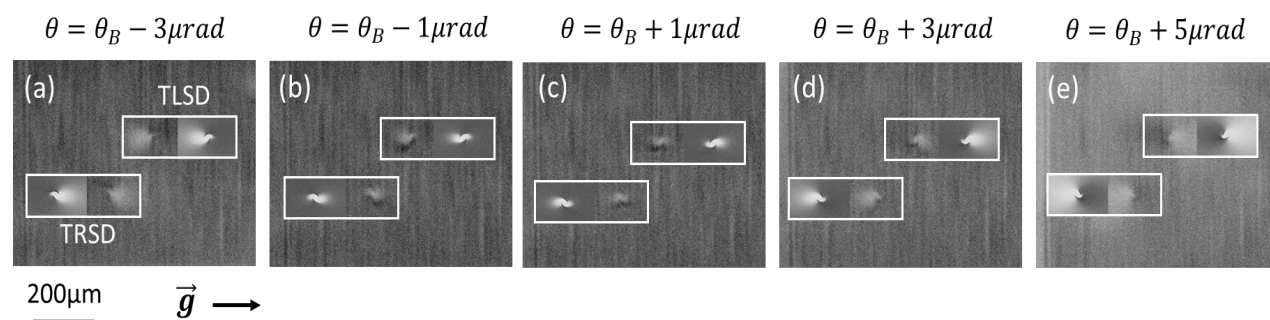

Figure 2. 4H-SiC 0008 rocking curve topographs of the same region. Five different diffraction conditions are noted by the θ (the angle between the incident X-ray and local diffraction plane) and Bragg angle θ_B. The variation of the dislocation contrast is shown in (a), (b), (c), (d) and (e) as the diffraction condition changes from $\theta_B-3\mu rad$ to $\theta_B+5\mu rad$. Ray tracing simulated image is placed alongside the topographic image in the box.

In addition to the contrast variations in back reflection topographs, we also observed changes of the contrast in synchrotron X-ray RCT. As the FWHM of 4H-SiC 0008 reflection in RCT is only around 2.4″, the contrast of the dislocations is much more sensitive to the diffraction conditions. Consequently, the sign of Burgers vector can be determined even using regular on-contour topographs. As shown in Fig. 2 (b) & (c), the diffraction condition is close to the perfect Bragg condition and the TSDs marked by the boxes have opposite sign of Burgers vector. More importantly, the contrast of the dislocation dramatically changes as the angle between the incident X-ray and local diffraction plane changes. As shown in Fig. 2 (a), $\theta = \theta_B$-3μrad, the white contrast 'fan' appears on the left if the dislocation is TLSD, while the white contrast is on the right for TRSD. Rocking the sample by 2 μrad, the white contrast becomes smaller for both TRSD and TLSD. As the sample continues to be rocked until $\theta = \theta_B$+5μrad (Fig. 2 (e)), the white contrast 'fan' becomes bigger on the right side of TLSD and to the left side of TRSD. Ray tracing simulated images placed alongside the topographic images correlate well, indicating that the contrast can be well described by orientation contrast mechanism.

Summary

4H-SiC dislocation contrast in weak beam synchrotron back reflection topography and RCT has been investigated in this study. The sign of Burgers vector can be determined in weak beam back reflection topograph and RCT using ray tracing simulations. The contrast of TSDs is observed to gradually change as the angle between the local diffraction plane and the incident beam changes. All these topographic images in weak beam topography can be simulated using ray-tracing method, indicating that under weak diffraction conditions, orientation contrast mechanism significantly contributes to the formation of the dislocation contrast.

Acknowledgement

References

[1] B. K. Tanner, D. K. Bowen, Synchrotron X-radiation topography, Mater. Sci. Rep. 8 (1992) 369-407

[2] A R Lang, 26 (1993) J. Phys. D: Appl. Phys. A1-A8

[3] F. Zontone, L. Mancini, R. Barrett, J. Baruchel, J. Hirtwig, Y. Epelboin, J. Synchrotron Rad. (1996). 3, 173-184

[4] J. Baruchel, M. D. Michiel, T. Lafford, P. Lhuissier, J. Meyssonnier, H. Nguyen-Thi, A. Philip, P. Pernot, L. Salvo, M. Scheel, C. R. Physique 14 (2013) 208-220

[5] M. G. Tsoutsouva, V. A. Oliveira, D. Camel, J. Baruchel, B. Marie, T.A. Lafford, Acta Mater. 88 (2015) 112-120

[6] X. R. Huang, D. R. Black, A. T. Macrander, J. Maj, Y. Chen, M. Dudley, Appl. Phys. Lett. 91, 231903 (2007)

[7] H. Peng, T. Ailihumaer, Y Liu, B. Raghothamachar, X. Huang, L. Assoufid, M. Dudley, J. Appl. Cryst. (2021). 54, 1225-1233

[8]   H. Matsuhata, H. Yamaguchi, T. Ohno, Philos. Mag. 92: 36, (2012) 4599-4617

[9]   X.R. Huang, M. Dudley, W.M. Vetter, W. Huang, S. Wang, C. H. Carter, Jr., Appl. Phys. Lett. 74 353 (1999)

[10]   J. W. M. DuMond, Phys. Rev. 52, 872 (1937)

[11]   X. R. Huang, M. Dudley, W. M. Vetter, W. Huang, W. Si, C. H. Carter Jr, J. Appl. Cryst. (1999). 32, 516-524